

EARTHQUAKE RESISTANCE BEHAVIOR OF CFT COLUMNS

Hiroyoshi TOKINOYA¹, Akiyoshi MUKAI², Kenzo YOSHIOKA³, Toshiyuki FUKUMOTO⁴, Takashi NOGUCHI⁵, Yoshiyuki MURATA⁶ And Yoshinari TANAKA⁷

SUMMARY

A five-year research program on concrete-filled steel tubular (CFT) systems started in 1992 as a part of the U.S.-Japan Cooperative Earthquake Research Program. A Japanese CFT Subcommittee of the program carried out the tests of stub-columns, beam-columns and beam-column connections using high strength steel and concrete. This paper presents the results of the beam-columns tests and discusses the ultimate strength and the deformation capacity. Consequently the models for the skeleton curves were proposed.

INTRODUCTION

In Japan, many tests of CFT beam-columns have been carried out since '60. Various combination of material strength become possible recently, however CFT beam columns using high strength steel and concrete has not been investigate sufficiently. Furthermore, most of the beam-columns tests were carried out under a constant axial load, thus there is no data on the beam columns subjected variable axial load or tensile axial load, which may be caused by overturning moment during earthquake. In the case of square section beam columns, the behavior under the two-dimensional lateral loads has not been investigated experimentally. The Japanese CFT Subcommittee considered the above state and conducted the tests program, which considered variety of material strength including high strength material, the axial loading condition and the lateral loading direction for square section beam-columns as the test parameters. This paper presents test results on beam-column tests subjected to combined vertical and horizontal loads, and discusses the ultimate strength and the deformation capacity, consequently derives the skeleton curve model for the restoring force characteristics.

EXPERIMENTAL PROGRAM

Test Specimens and Parameters:

Figure 1 shows the details of specimens. Heavy stubs made of CFT were attached at both ends to guarantee large stiffness sufficiently. The steel tube is through the stubs and welded there. The clear column length is $6D$, and the shear span is $3D$, where D is column depth or diameter. Square tube specimens were fabricated by welding together two pieces of channel sections, which were cold press formed from flat plate. Circular tube specimens were cold formed by press bending. Table 1 shows the properties of the specimens. The test parameters are steel tube cross section shape (square and circular), steel grade, width (diameter)-to-thickness ratio of steel tube, concrete grade, axial loading condition (constant and variable), and lateral loading direction for the square specimens (Biaxial-bending).

¹ Tech. Res. Inst., Obayashi Corp., Tokyo, Japan E-mail: tokinoya@tri.obayashi.co.jp

² Building Res. Inst., Ministry of Construction, Ibaraki Japan E-mail: mukai@kenken.go.jp

³ Daiichi Univ., Kagoshima, Japan E-mail: k-yoshioka@daiichi-koudai.ac.jp

⁴ Tech. Res. Inst., Kajima Corp., Tokyo, Japan E-mail: fukumoto@katri.kajima.co.jp

⁵ Tech. Res. Center, Aoki Corp., Ibaraki, Japan E-mail: TakashiNoguchi@aoki.co.jp

⁶ Tech. Res. Inst., Penta-Ocean Construction Co., Ltd., Tochigi, Japan Fax: +81-287-39-2133

⁷ Dai Nippon Construction, Tokyo, Japan E-mail: tanay@mb.infoweb.ne.jp

The steel grade is classified with tensile strength of steel plate before cold formed, which are 400 MPa (S400), 590 MPa (S590) and 780 MPa (S780). The yield strengths obtained by tension tests are listed in Table 1. The concrete grade is classified with design strength, which are 40 (C40) or 90 MPa (C90). The actual cylinder strengths are listed in table 1. Two classes of FA and FC were selected on the width (diameter)-to-thickness ratio D/t of steel tube, based on the classification of hollow steel tubes by Japanese Building Standard Law Enforcement Order [3]. Hollow steel tubes in FA class have smaller D/t ratio and have larger ductility as the structural members than tubes in FC class have. The constant compressive axial load is 40 % of $N_o (= {}_cA*_c\sigma_B + {}_sA*_s\sigma_y)$, where ${}_cA$ and ${}_sA$ are the sectional area of concrete and steel, respectively; and ${}_s\sigma_B$ is cylinder strength of concrete; and ${}_s\sigma_y$ is yield strength of steel plate. The variable axial load is within the range of 30 % tension of $N_s (= {}_sA*_s\sigma_y)$ to 70 % compression of N_o . The lateral loading direction is angle of 22.5 or 45 degrees to the principal axis of the square column section. The number of the square tube specimens is twenty, which includes four specimens subjected to variable axial load and four ones subjected to Biaxial-moment, and that of the circular tube specimens is thirteen, which includes four specimens subjected to the variable axial load. The total of all specimens is thirty-three.

Test Setup and Procedure:

Fig. 2 and 3 shows the test setup and the rule on the cyclic horizontal loading, respectively. The test setup, which consists of two vertical hydraulic actuators and one horizontal actuator, is designed to subject specimen to an axial load and horizontal deformation. The two vertical actuators apply the axial load and keep the upper stub in parallel to lower one as well. The horizontal actuator applies the horizontal load in the displacement control mode. Fig. 4 shows the rules on the axial load. For the specimens subjected to the variable axial load, the compressive axial load of 70 % of N_o is maintained constant during the positive horizontal displacement, while the tension axial load of 30 % of N_s is maintained constant during the negative displacement. The axial load is changed when the horizontal displacement is zero while the horizontal load is maintained zero, permitting the horizontal drift happening.

EXPERIMENTAL RESULTS AND DISCUSSION

The test results are summarized in table 1. The test maximum flexural strength ${}_cM_u$ is the column end moment in the horizontal loading direction, including the $P-\Delta$ moment. The calculated ultimate flexural strength ${}_cM_u$ is the ideal full plastic state moment based on the rectangular stress blocks assumed for steel tube and concrete, where the intensity of stress is equal to yield strength ${}_s\sigma_y$ and the cylinder strength ${}_c\sigma_B$, respectively. For the specimens subjected to variable axial load, each of ${}_cM_u$ and ${}_cM_u$ are obtained both in the positive loading with 0.7 N_o compressive axial load, and in the negative loading with tension axial loading, respectively. The test limit rotation ${}_cR_u$ expresses the rotation angles where restoring force of the specimen decreased to 95 % of the maximum one. The rotation angle R is the end rotation angle in the horizontal loading direction, which is obtained from dividing the measured horizontal drift by the clear column length. The calculated limit rotation ${}_cR_u$

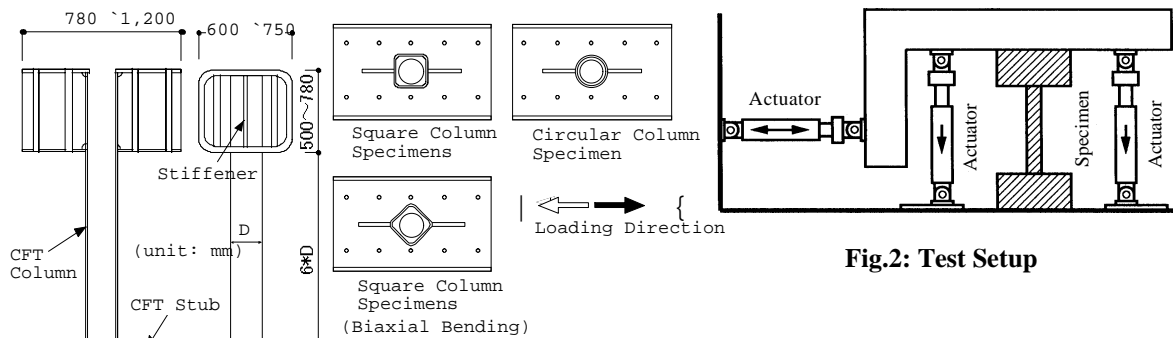


Fig.2: Test Setup

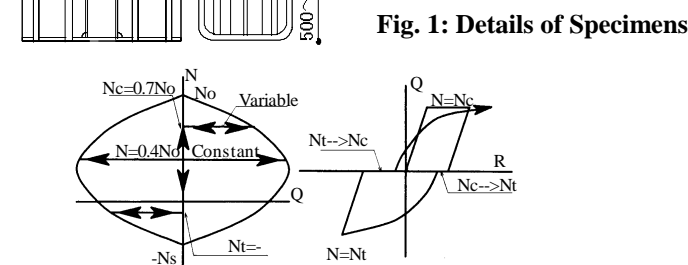


Fig. 1: Details of Specimens

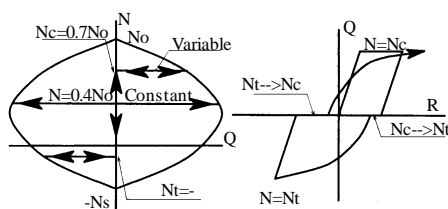


Fig. 4: Axial Loading Rules

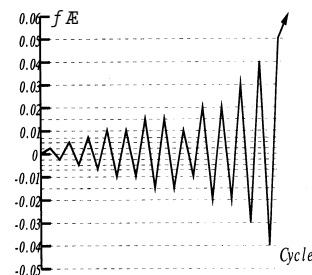


Fig.3: Horizontal Loading History

Table 1: Summary of Specimens and Tests Results

Specimen	Cross Section			Tests Parameters						Max. Strength			Limit Rotation				
	Shape	D mm	t mm	Steel Grade	$s\sigma_y$ MPa	D/t (rank)	Con. Grade	$c\sigma_B$ MPa	Axial Load	eM_u kNm	cM_u kNm	eM_u kNm	eR_u %	cR_u %	eR_u %		
SC4A4C	Circle	241	4.7	S400	284	51 (FC)	C40	39.2	0.4No	173	114	1.52	4.54	3.66	1.24		
SC4A9C		238								C90	88.2	202	160	1.26	1.97	3.12	0.63
SC6A4C		241	9.0	S590	482	27 (FA)	C40	35.5	0.4No	371	242	1.53	4.68	4.64	1.01		
SC6A9C		241								C90	84.4	422	300	1.41	3.92	4.05	0.97
SC6A9V		241								C90	91.7	274	208	1.32	3.12	1.96	1.59
SC6C4C		238	4.5	S590	504	53 (FC)	C40	35.5	0.4No	220	144	1.53	2.92	3.14	0.93		
SC6C9C		240								C90	84.4	254	211	1.20	1.56	2.99	0.52
SC6C9V		241								C90	91.7	153	159	0.96	1.39	0.90	1.55
SC8A4C		161	9.1	S780	819	18 (FA)	C40	35.5	0.4No	245	156	1.57	4.10	5.05	0.81		
SC8A9C		161								C90	93.9	261	178	1.47	4.40	4.33	1.02
SC8A9V		161								C90	93.9	173	111	1.56	3.10	2.40	1.29
SC8C9C		160	4.8	S780	771	34 (FC)	C40	35.5	0.4No	151	113	1.34	2.00	3.72	0.54		
SC8C9V	159	C90								93.9	110	77	1.43	2.00	1.72	1.16	
SR4A4C	Square	210	5.8	S400	294	36 (FA)	C40	39.2	0.4No	187	135	1.39	1.40	1.67	0.84		
SR4A9C		210								C90	88.2	225	187	1.20	1.32	1.53	0.86
SR4C4C		210	4.5	S400	276	47 (FC)	C40	39.2	0.4No	151	114	1.32	1.00	1.29	0.78		
SR4C9C		209								C90	88.2	202	163	1.24	0.85	1.18	0.72
SR6A4C		211	8.8	S590	536	24 (FA)	C40	39.3	0.4No	373	278	1.34	2.51	2.51	1.00		
SR6A9C		211								C90	88.3	402	336	1.20	2.21	2.30	0.96
SR6A9V		210								C90	91.7	259	209	1.24	1.41	1.36	1.03
SR6C4C		211	6.0	S590	540	36 (FC)	C40	39.3	0.4No	263	218	1.21	1.93	1.69	1.14		
SR6C9C		210								C90	93.7	295	278	1.06	1.43	1.53	0.93
SR6C9V		212								C90	91.7	163	187	0.87	0.94	0.91	1.03
SR8A4C		178	9.5	S780	824	19 (FA)	C40	42.3	0.4No	345	270	1.28	2.97	2.97	1.00		
SR8A9C		179								C90	94.5	377	317	1.19	2.91	2.74	1.06
SR8A9V	178	C90								94.5	217	170	1.28	1.86	1.67	1.12	
SR8C4C	180	6.7	S780	823	27 (FC)	C40	42.3	0.4No	240	223	1.08	2.00	2.12	0.94			
SR8C9C	180								C90	94.5	264	267	0.99	2.00	1.96	1.02	
SR8C9V	180								C90	94.5	146	155	0.94	1.07	1.18	0.91	

S R 6 A 9 C 45
a b c d e f g

- a : Beam-Column Test
- b : Shape of Column Section, C- Circle section, R- Square section
- c : Steel Grade, 4-S400, 6-S590, 8-S780
- d : Width (Diameter)-to-thickness ratio, A-FA rank,C-FC rank
- e : Concrete Grade, 4-C40, 9-C90
- f : Axial Load Ratio, C-Constant(0.4No), V-Variable(0.7No to -0.3Ns)
- g : Loading Angle, 45-45 degree, 22.5-22.5 degree

is obtained from the proposed formulae described in the following section. Fig 5 ~ 8 show the relationships between the end moment M and the rotation angle R, and relationships between the axial strain ϵ and the rotation angle R, respectively. The axial strain ϵ means the average strain over the column length. The relationships between the test parameters and the test results of the flexural strength (eM_u/cM_u), and the limit rotation angle eR_u were shown in Fig. 9. As to the strength and deformation capacity, the following observation was made, where the deformation capacity here is defined as the limit rotation angle as described above.

Square Columns:

For all the specimens, the maximum flexural strength was observed after the local buckling occurred in the compressive flange. After the local buckling, axial strain increased drastically.

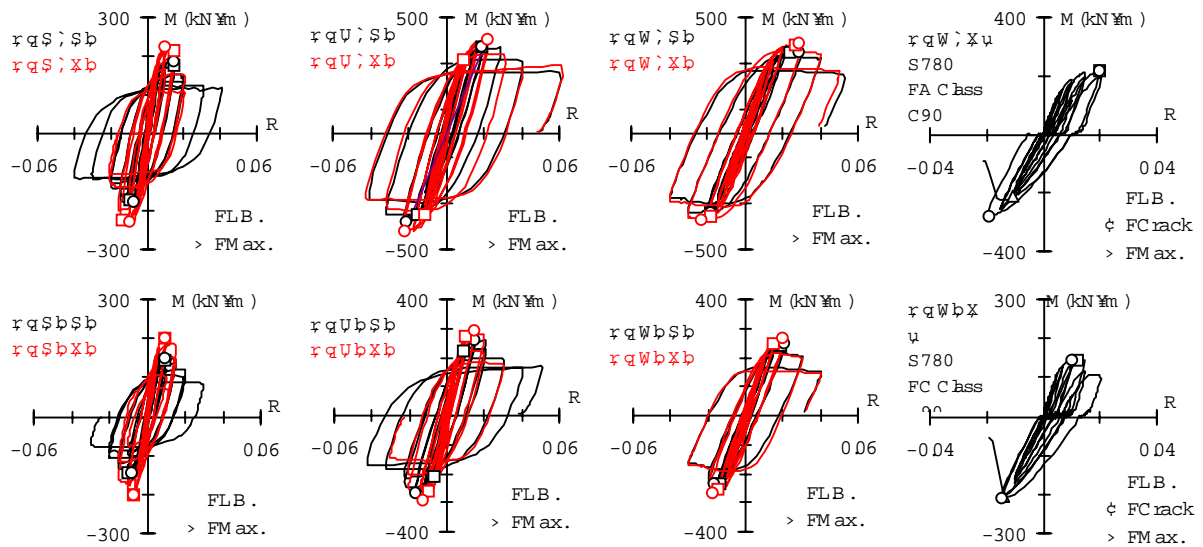


Fig. 5: Moment-Rotation Angle Relationships of Square Columns Specimens Loaded in the Direction in the Angle of Zero degree

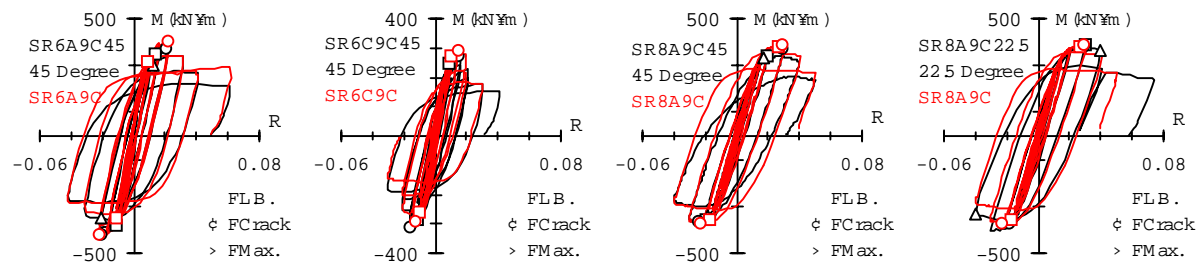


Fig.6 Moment-Rotation Angle Relationships of Square Columns Specimens Loaded in the Direction of the Angle of 22.5 degree and 45 degree

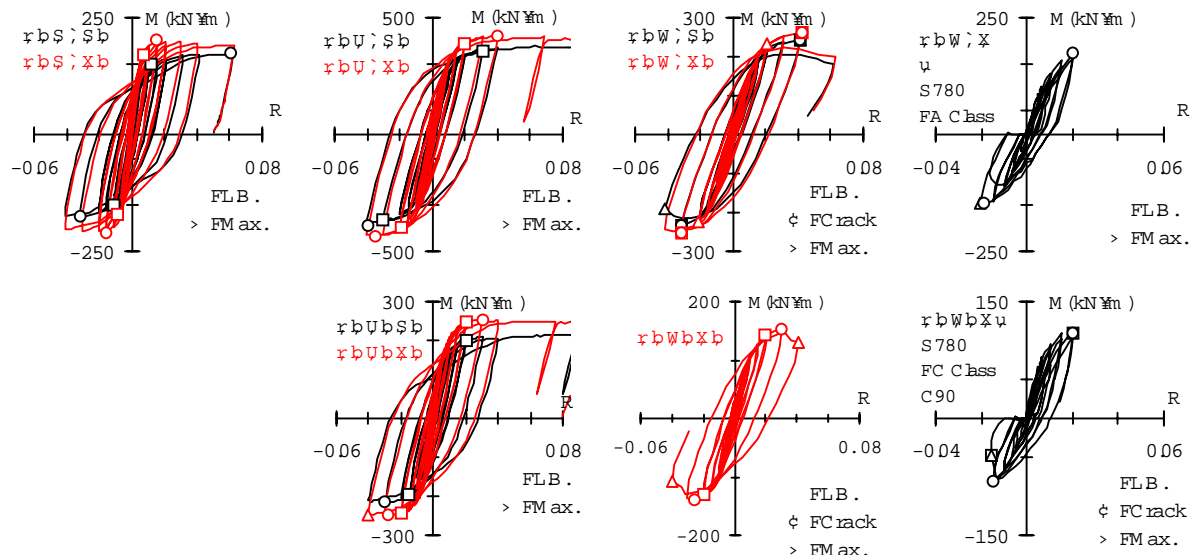


Fig. 7: Moment-Rotation Angle Relationships of Circular Columns Specimens

As to the specimens under constant compressive axial load, no crack occurred in steel tube. The ratios of eM_u/cM_u were 0.99~1.39, which were higher as steel grade became lower or concrete grade became lower as well. D/t ratio of steel tube had little influence on the ratio of eM_u/cM_u . The deformation capacity became larger as the steel grade became higher. However, concrete grade has little influence on the deformation capacity. This indicates that steel tube of high strength steel or thick plate is effective to improve brittle behavior of high strength concrete, and that the effect of restraining local buckling of steel tube by the filled concrete does not depend on concrete strength. The axial strain ϵ became larger as the concrete grade became higher, as the steel grade became lower and as D/t ratio became larger.

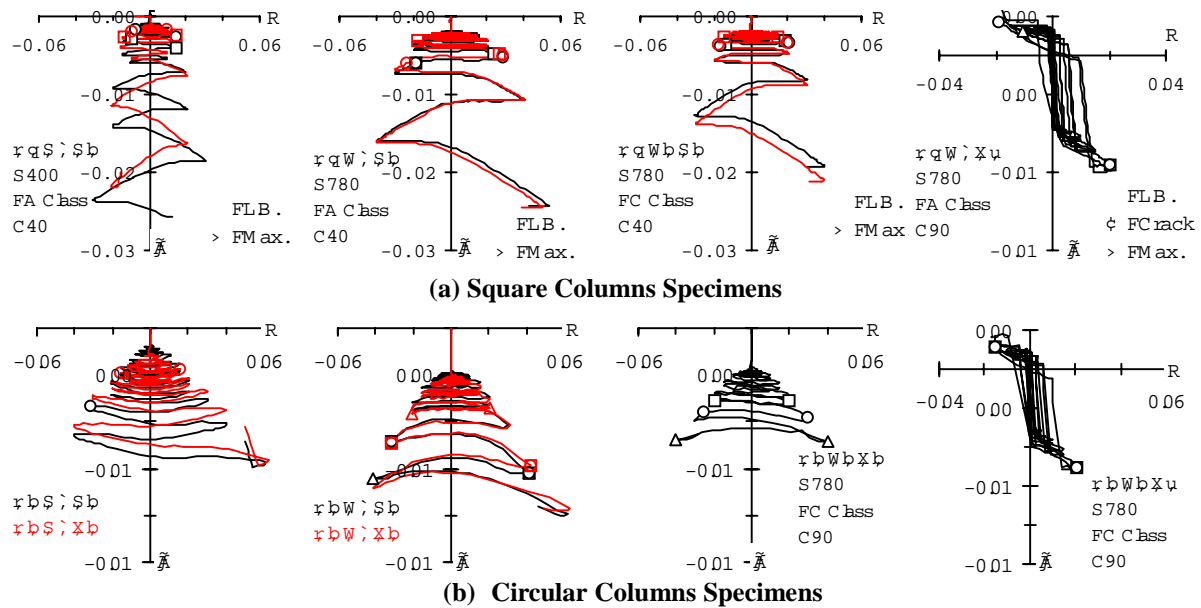


Fig. 8: Rotation Angle-Axial Strain Relationships

As to the specimens under Biaxial-bending moment, in the specimens of S590 with FA class and all specimens of S780, cracks occurred at steel tube corner. The steel tube corner has been experienced plastic strain in cold forming and bears severe stress, and then these may cause the cracks. The cracks however did not cause any drastic strength reduction. The maximum flexural strengths were the same as that of specimens under Uniaxial-bending. The behavior was also very similar to that of specimen under Uniaxial-bending. This indicates that square columns have the almost same performance in any lateral loading directions.

As to the specimens subjected to variable axial load, local buckling was observed at early deformation stage in positive horizontal loading with compressive axial loading. Then cracks occurred in negative horizontal loading with tension axial loading. The strength of the specimens with S590 and S780 with FC class did not reach the calculated ones because of crack. The compressive flange in loading direction of compressive axial loading is also tensile flange in the loading direction with tension axial loading, and then the deformation capacity and the strength were smaller than constant axial loading specimens.

Circular Columns:

The maximum flexural strengths of all specimens were observed after the local buckling occurred in the compressive flange. Although after the local buckling, neither drastic strength reduction nor axial strain increment was observed. The maximum strengths eM_u of all specimens under constant axial load exceeded the calculated strengths cM_u , and that the ratio of eM_u/cM_u was higher than that of the square columns. The crack occurred in the specimens under constant axial loading, one with S590 and all with S780, but it did not cause any drastic strength reduction.

The same tendency in the ratio of eM_u/cM_u was observed as in the case of the square columns that is, the material strength affected on the ratio, but the D/t did not affect. On the other hand, in the deformation capacity, the different tendency was observed, i.e. the steel grade did not affect on it and the concrete grade affected in the circular columns. Effects of D/t on the deformation capacity were observed as well in the circular columns.

As to the specimens subjected to variable axial load, the ratio of eM_u/cM_u and the deformation capacity were less than others, because of the early cracking under tensile axial load.

FORMULAS OF SKELETON MODEL

The skeleton curve of relationship between moment and rotation angle of CFT beam-column under constant axial load can be modified to a tri-linear type as shown in Fig. 10. This model is determined by five parameter: the elastic stiffness K_e , the stiffness degrading ratio α_y , the yield moment M_y , the ultimate moment M_u and the limit rotation angle R_u . The M_y is the short-term allowable strength [1]. The M_u is the ultimate strength proposed by Sakino et al. [2], using as well results of stub-columns tests conducted as the U.S-Japan cooperative program,

where the confining effect is considered on circular column and the local buckling effect is considered on square column. The α_y and the R_u were derived by statistically processing the experimental data as described in section mark of 4.1 and 4.2, respectively. These data included not only the test results obtained in U.S.-Japan research but those reported in Japan. The main properties of processed data except U.S.-Japan research were shown in

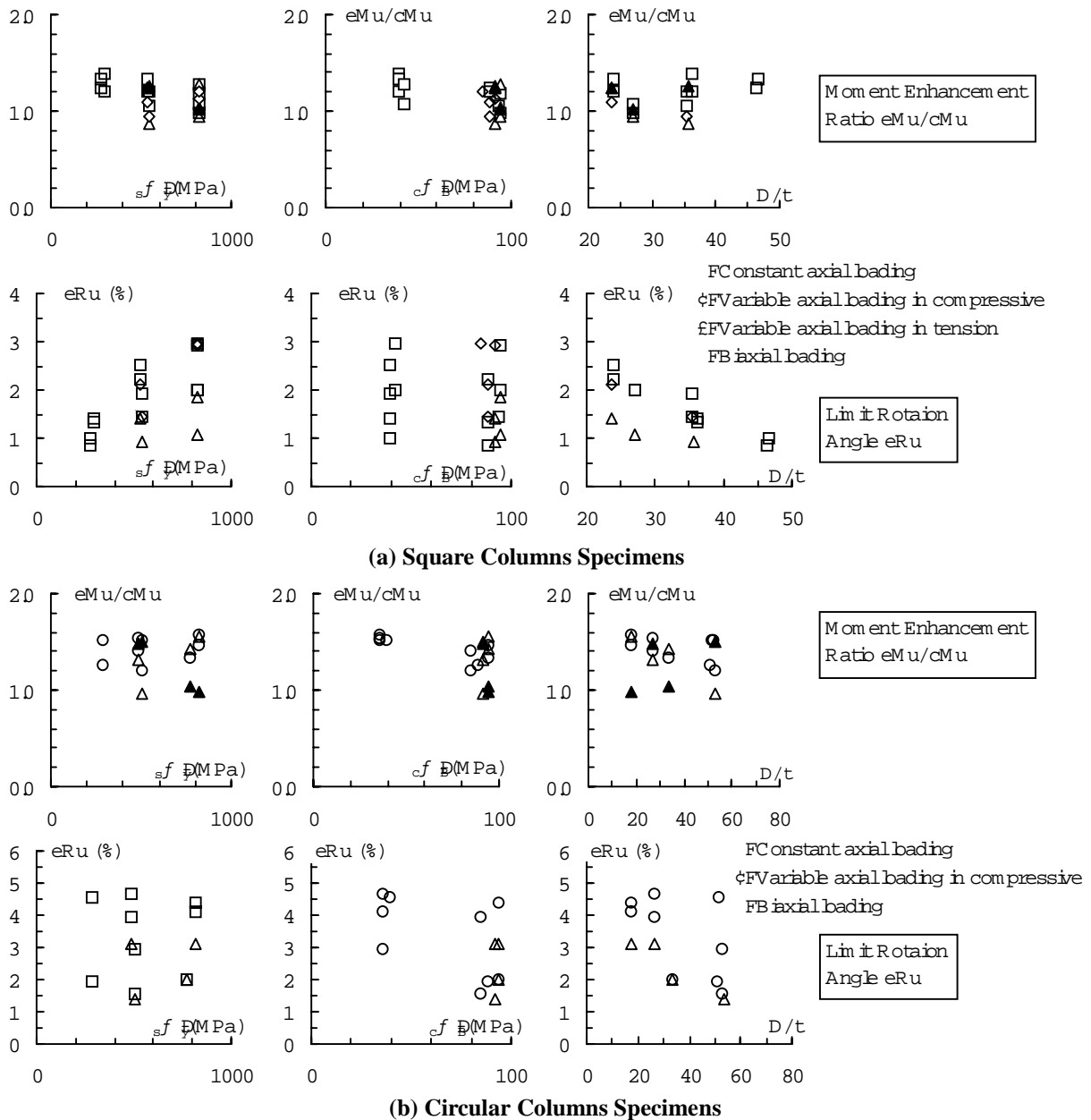


Fig. 9: Experimental Parameters Effects on eMu/cMu and eRu

table 2. α_y is defined as $K2/K1$ as illustrated in Fig. 11, where both of $K1$ and $K2$ were determined by the experimental data. $K1$ was a secant modulus at the point of one-third of the maximum moment, and $K2$ was a secant modulus at the point of 85% of the maximum moment, respectively. R_u is defined as the rotation angle at which restoring force reduced to 95% of the maximum one. In this study, restoring force is considered instead of moment, so that instability caused by P- Δ effect can be considered directly. A series of regression analysis is carried out to research correlation between α_y and the properties listed in table 2, and one between R_u and the properties, respectively.

Stiffness Degrading Ratio α_y :

As the results of regression analysis, none of properties appeared high correlation between α_y , in both the square columns and the circular columns. 80 % of α_y distributed in range of 0.4~0.9 in spite of the section shape.

Consequently, α_y can be estimated as 0.70 for square columns, while as 0.65 for circular columns, which are the averaged values of the data, respectively.

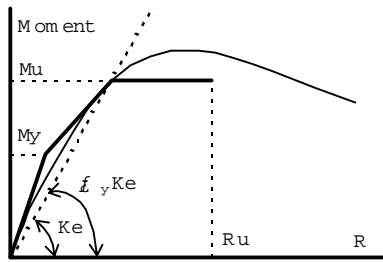


Fig.10: Model of Moment-Rotation Angle Relationship

Ke : Elastic Stiffness
 α_y : Stiffness Degrading Ratio
 My : Calculated by [1]
 Mu : Calculated by [2]
 Ru : Limit Rotation Angle

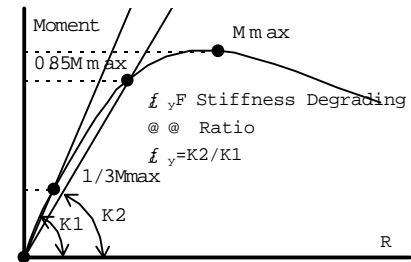


Fig.11: Definition of α_y Derived from Experimental Results

Table 2: Range of Referenced Experimental Data except the U.S.-Japan data

Theme	Stiffness Degrading Ratio		Limit Rotation Angle	
	Square	Circle	Square	Circle
n	108	45	151	55
D/t	15.6 ~ 70.0	20.4 ~ 77.0	13.8 ~ 95.0	16.7 ~ 66.7
$c\sigma_y$	194 ~ 642	283 ~ 549	194 ~ 786	295 ~ 549
$c\sigma_B$	20.0 ~ 102	28.0 ~ 84.9	17.6 ~ 102	17.2 ~ 128
N/No	0.0 ~ 0.83	0.0 ~ 0.7	0.0 ~ 0.9	0.1 ~ 0.8
a/D	1.5 ~ 5.3	1.8 ~ 5.2	1.5 ~ 5.7	1.8 ~ 5.0

Notes: n: the number of processed data except the U.S.-Japan data

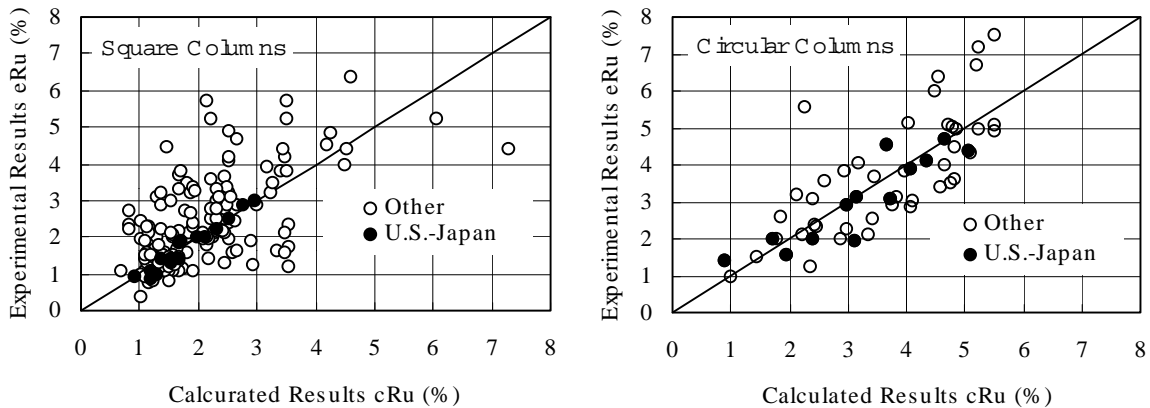


Fig. 12: Comparison Calculated Limit Rotation Angle cRu between Experimental Limit Rotation Angle eRu

Limit Rotation Angle R_u :

As the results of regression analysis, the limit rotation angle R_u for the square columns can be written

$$Ru(\%) = \frac{100}{0.15 + 3.79 \frac{N}{No}} \cdot \frac{t}{D} \cdot \beta \tag{1}$$

in which, $\beta = 1.0 - \frac{c\sigma_B - 40.3}{566} \leq 1.0$ ($c\sigma_B$: MPa)

, and while for the circular columns can be written as follow.

$$Ru(\%) = 8.8 - 6.7 \times N / No - 0.04 \times D / t - 0.012 \times c\sigma_B \tag{2}$$

These formulae were established considering follows: The parameters of the axial ratio N/No and the width (diameter)-to-thickness ratio D/t had high correlation between the R_u , both in the square columns and in the circular columns. Thus, R_u increased with decrease of N/No or decrease of D/t; Further in the circular columns, the concrete strength $c\sigma_B$ had also high correlation, that is, R_u increased with increase of $c\sigma_B$. These tendency was observed in the U.S.-Japan tests results described in above section mark of 3.1 and 3.2 except of the steel tube

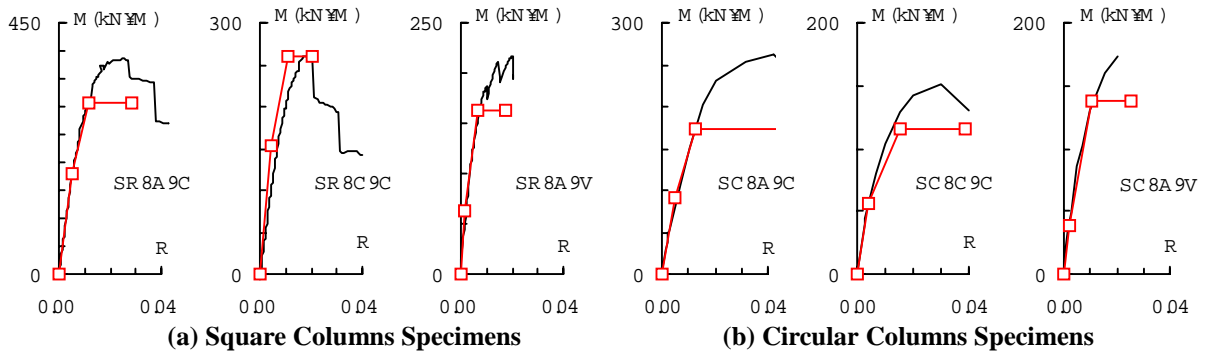


Fig. 13: Comparison Proposed Skeleton Model between Experimental Enveloped Curve

strength effects on R_u of the square columns. $s\sigma_y$ had influence on R_u of the square columns in the U.S.-Japan tests, however it was not observed from the regression analysis. It was mainly because data except the U.S.-Japan tests included much kind of steel tube manufactured by several methods. Fig. 12 shows the relationship between the experimental limit rotation angle ${}_cR_u$ and the calculated ones ${}_cR_u$ estimated by the equation (1) or (2). The coefficient of correlation is 0.67 for whole data in square columns, and that is 0.83 in circular columns, while the coefficient for the U.S.-Japan data is particularly high in the both the square columns and the circular columns.

Enveloped Curve Model:

Fig. 13 shows the skeleton curves estimated by the proposed five-parameter model as to the selected specimens expressed by red line, comparing with the experimental results expressed by black line. The proposed models estimated the experimental enveloped curves lower beyond the second corner point. However, the hysteretic loop area in the rotation angle range over 1%, supposing the normal tri-linear hysteretic rule, is about 70% of that of the experimental results. The reason for this tendency is that the unloading stiffness in the normal tri-linear hysteretic rule is higher than that of the experimental loop.

CONCLUSIONS

The following conclusions are obtained from the experimental investigations and statistically processing experimental results reported in Japan on the beam-columns tests.

- 1) The circular columns have greater ultimate flexural strength and deformation capacity than the square columns.
- 2) The columns under variable axial load have lower ultimate flexural strength and lower deformation capacity than those under constant axial load, respectively.
- 3) Square columns have almost the same performance in any lateral directions
- 4) The larger width (diameter)-to-thickness ratio and the higher axial load ratio reduced the deformation capacity

ACKNOWLEDGEMENT

The CFT research presented in this paper was conducted by the members of the CFT Subcommittee in Japan side, chaired by Prof. Shosuke Morino, Mie University. The steel tube was prepared by the KOZAI Club. The series of tests were jointly carried out at the following research institute: BRI of Ministry of Construction, T.R.I of Asanuma Co., T.R.I. of Aoki Co., T.R.I of Obayashi Co., T.R.I. of Kajima Co., T.R.I. of Matsumura Co., T.R.I. of Hazama Co., T.R.I. of Penta-Ocean construction Co. and T.R.I of TOYO Construction. The authors wish to express sincere gratitude to the members of the subcommittee and the other persons related.

REFERENCES

1. Architectural Institute of Japan (1987), *AIJ Standards for Structural Calculation of Steel Reinforced Concrete Structures*.
2. Sakino, K. and Ninakawa, T. (1998), "Estimation Method for Ultimate Moment of Circular CFT Columns", *Summaries of Technical Papers of Annual Meeting of AIJ, Structures 3*, pp1229-1230.
3. The Building Center of Japan (1991), "Guideline to structural calculation under the building standard law", 190pp.